PLASMA WAVES AT THE DAYSIDE MAGNETOPAUSE

J. LABELLE and R. A. TREUMANN

Max-Planck-Institut für Extraterrestrische Physik, 8046 Garching bei München, B.R.D.

(Received 28 March, 1988)

Abstract. Experimental investigations of plasma waves at the magnetopause, including recent results from the AMPTE/IRM satellite, show that both δE and δB fluctuations typically have a featureless spectrum which monotonically decreases with frequency; integrated rms amplitudes are typically a few mV m^{-1} for δE and 10 nT for δB, though in particular δE can be as much as an order of magnitude larger in exceptional cases. Surveys show a lack of correlation between wave parameters and the magnetopause parameters. Under the assumption that crossing the diffusion region would give a pronounced signature in the waves, the survey data allow an upper limit to be placed on the latitudinal extent of the diffusion region, which is about 1000 km – implying that it is not surprising that the wave data surveys have so far failed to detect it. The observed wave turbulence levels have been used to estimate diffusion coefficients under different assumptions for the wave mode, but the resulting diffusion coefficient is always too small to explain either reconnection or boundary layer formation. Recent work of Galeev *et al.* (1986) indicates that the dominant diffusion process may be 'magnetic field migration', which is a macroscopic process involving the interaction of tearing mode islands. Assuming this mode to be present at the observed level of δB, a particle diffusion coefficient of nearly 10^9 m^2 s^{-1} is obtained. Another macroscopic diffusive process which could occur at the magnetopause is stochastic $\mathbf{E} \times \mathbf{B}$ scattering, which also implies a diffusion coefficient the order of 10^9 m^2 s^{-1} if the observed δE spectrum is assumed to be a turbulent cascade consisting of convective cells.

1. Introduction

The outer boundary of the Earth's magnetosphere has naturally aroused interest ever since the concept of the magnetosphere became known. The earliest satellites to explore the magnetopause regions resulted primarily in an understanding of the macroscopic shape of this boundary, and to some extent its changes with time. Its shape and standoff distance are in good agreement with those expected from hydrodynamic considerations of the pressure balance between the solar wind and the magnetosphere.

Since the early days, a great deal has been learned by ever more sophisticated satellites which penetrated the magnetopause region. In particular, the dayside magnetopause has proven to be a very dynamic region. A significant amount of evidence has arisen which indicates that the dayside magnetopause is the site for magnetic reconnection during times when there exists a large angle between the earth's magnetic field and the interplanetary field (IMF). This evidence comes in the form of satellite observations of high speed plasma flows which are consistent with fairly continuous reconnection along the boundary near the satellite location (Paschmann *et al.*, 1979, 1982; Sonnerup *et al.*, 1981) and satellite observations of structures in the magnetic field and particles which are signatures of intermittent events (Russell and Elphic, 1978). In addition, a boundary layer of mixed plasma exists at the magnetopause and is itself structured in a complicated way (e.g., Sckopke *et al.*, 1981).

Explanations for both these phenomena – reconnection and the boundary layer –

Space Science Reviews **47** (1988) 175–202.

imply an important role for microscopic plasma waves. We shall define microscopic plasma waves to be magnetic and electric field fluctuations with frequencies greater than 0.1 Hz in the satellite reference frame. A number of satellites have been equipped to measure waves in this frequency range, including most recently the AMPTE satellites IRM and UKS. In this review, we present in Section 2 a history of the wave spectral measurements at the dayside magnetopause, including the most recent (and until now not published) AMPTE/IRM results. In Section 3 we review surveys of the magnetopause plasma waves and discuss their implications for reconnection. In Section 4 we review recent theoretical advances and discuss their implications for both reconnection and boundary-layer formation.

2. Wave Spectral Observations

2.1. Magnetic field fluctuations

Fluctuations in the magnetic field were observed very early to be characteristic of the magnetopause. Many of the early studies concentrated on fast oscillations of the boundary itself, which were found to have periods ranging from 1–5 minutes (Holzer *et al.*, 1966; Hyde, 1967; Anderson *et al.*, 1968) to periods near ten seconds (Smith and Davis, 1970; Aubry *et al.*, 1971). Simulation studies of the nonlinear Kelvin–Helmholtz instability (Miura, 1987) have recently shown that these long-period oscillations with periods of 1–6 minutes can be driven by the Kelvin–Helmholtz instability. Their typical wavelengths are of the order of $2–8R_E$ and is consistent with the eddy turbulent structure of the low-latitude boundary layer reported by Sckopke *et al.* (1981).

One of the earliest attempts to measure the spectrum of magnetic fluctuations is due to Holzer *et al.* (1966). They show typical spectra from the outer magnetosphere, quiet- and noisy-magnetosheath, and the solar wind, but do not specifically investigate the magnetopause. Cummings and Coleman (1968) present a magnetic field spectrum just outside the magnetopause. They obtain the dependence $I_m \equiv \delta B^2/2\mu_0 \sim f^{-2}$ over the frequency range 0.2–0.8 Hz, with an integrated amplitude of about 10 nT over this range. Aubry *et al.* (1971) observe waves near the magnetopause boundary with frequency near 0.5 Hz and an amplitude of 10 nT. Fairfield (1971) reviews several magnetopause crossings by the IMP-6 satellite which show waves near 0.5 Hz with amplitudes varying from 4–10 nT. Thus, these early satellite measurements are in agreement with wave amplitudes the order of ≤ 10 nT for the below 1 Hz frequency regime.

Neugebauer *et al.* (1974) report on magnetic field waves at the magnetopause observed with the OGO-5 satellite. They note waves in the vicinity of the ion-cyclotron frequency ($f_{ci} \approx 1$ Hz) of amplitude 1–10 nT. They also use a searchcoil to determine the waves in the 10–1000 Hz frequency range. In this frequency range, they report that the spectrum at the magnetopause resembles that in the outlying sheath, which is characterized by approximately an f^{-3} power law in their data. Bahnsen (1978) reports measurements from HEOS-2 in the frequency range 20–235 Hz. The wave amplitude clearly peaks in the magnetopause region, and the power spectral densities fall off with

increasing frequency. Hansen *et al.* (1976) had previously reported such peaks in the cusp-sheath interface region, also using HEOS-2 data.

The ISEE mission produced a wealth of data concerning plasma waves in the magnetopause region. Gurnett *et al.* (1979) observed magnetic field waves in the frequency range 5.6–1000 Hz which are characterized by a $f^{-3.3}$ power spectrum and an integrated amplitude of 1.3 nT. Tsurutani *et al.* (1981) examined many magnetopause crossings and refined the results of Gurnett *et al.*, finding that the typical spectrum is defined by $I_m = 10f^{-3.9}\ \mathrm{nT^2\ Hz^{-1}}$, but with as much as an order of magnitude difference in amplitude from case to case. Anderson *et al.* (1982) identified the wave morphology of the magnetopause current layer, the boundary layer, and flux-transfer-events and found that all three have very similar wave characteristics. They identified a 'turbulent region' near the magnetopause, characterized by waves near 1 Hz with amplitudes of about 10 nT.

This turbulent region may be identical to that identified by Perraut *et al.* (1979), based on the relatively unusual times when the magnetopause penetrates to the geosynchronous orbit of GEOS-2. They observed a turbulent layer roughly 500 km thick characterized by magnetic field waves of up to 10 nT amplitude in the frequency range 0.3–11 Hz; the amplitude is greatest near the current layer and rolls off as the satellite moves away from the magnetopause. Rezeau *et al.* (1986) extended the work of Perraut *et al.* (1979) by determining typical spectral indices in the 0.5–11 Hz frequency range. They reported $I_m \sim f^{-2.5}$, in agreement with Cummings and Coleman (1968) but somewhat shallower than the spectral index which has been reported at higher frequencies, indicating perhaps that there is a break in the spectrum near 10 Hz.

The AMPTE/IRM magnetopause observations display all of the previously observed characteristics. Figure 1 shows three magnetopause crossings which occurred within a 6 min interval on October 9, 1984. At the left side of the figure (14:18 UT), the satellite is in the magnetosphere, as is clear from the high temperature at low density. The magnetic field is expressed in LMN coordinates (Russell and Elphic, 1978). About 14:20 UT, the field changes direction dramatically, while simultaneously the temperature decreases and the density rises to around 10 $\mathrm{cm^{-3}}$, a value typical for the magnetosheath. At 14:22 UT, the satellite makes a rapid exit from the sheath into the boundary layer, and then quickly enters the sheath again. Near 14:23 UT, the satellite encounters a diamagnetic structure which we identify as a magnetic 'hole' similar to that shown by Lühr and Klöcker (1987) and Treumann *et al.* (1986). During the three magnetopause crossings, the plasma flow reaches very high values, which Paschmann *et al.* (1986) show to be consistent with the expected signature of reconnection occurring along the magnetopause at some distance (though not too far) from the satellite. The top two pannels are gray-scale representations of the 0–16 Hz magnetic field fluctuations and the 30 Hz–10 kHz electric field fluctuations. The magnetic fluctuations are the order of 10 nT. The magnetic turbulence clearly favors the part of the magnetosheath to the magnetosphere, and falls off at further distances from the boundary; this region of magnetic turbulence is, therefore, similar to the turbulent layer identified by Perraut *et al.* (1979) and other authors. Although it may be important for the formation of the

boundary layer, this magnetic turbulence layer is not identical with the boundary layer. In fact, at the time shown in Figure 1, the boundary layer is either extremely thin or completely absent, since the plasma characteristics switch from magnetospheric plasma to sheath plasma exactly at the current layer, as noted by Paschmann *et al.* (1986).

Figure 2 shows the spectrum of magnetic field fluctuations at or just outside the magnetopause as reported by many observers and serves as a summary of this section. The spectrum measured with the AMPTE/IRM during the first magnetopause crossing of Figure 1 is also indicated. Although the figure contains measurements from different instruments sampling different latitudes, local times, and radial distances of the dayside magnetopause for times as great as ten years apart, a remarkably consistent picture arises: almost all of the observed wave power (δB) corresponds to frequencies near or below 1 Hz, with the spectrum falling off at higher frequencies as $f^{-\alpha}$, $\alpha \approx 3$–4. The integrated amplitude is approximately 10 nT, with 90% of that amplitude at frequencies below 10 Hz. The various measurements all agree with one another, within an order of magnitude in power, which is the typical variation of the spectra from example to example (Tsurutani *et al.*, 1981).

2.2. Electric field fluctuations

Measurements of the wave electric field for frequencies above 10 Hz have been made using double-probe detectors combined with filter banks or swept frequency analysers. Scarf *et al.* (1974) described OGO-5 wave observations of the cusp-magnetosheath interface for a very disturbed day. The outbound magnetopause crossing is associated with an increase in the 0.56–70 kHz wave intensities to integrated amplitudes near 1 mV m^{-1}. Rodriguez (1979) performed a comprehensive survey of electric field turbulence in the magnetosheath using IMP-6 data and found typical amplitudes of about 1 mV m^{-1} over the frequency range 20 Hz–70 kHz. He noted examples of spike-like electrostatic waves near the magnetopause.

Gurnett *et al.* (1979) studied examples of waves at the magnetopause measured using the ISEE satellites. They measured typically a featureless spectrum of electric field turbulence which varies as $f^{-2.2}$ over the frequency range 5.6 Hz–100 kHz, with a broadband amplitude of about 5 mV m^{-1} over this range. This broadband amplitude is somewhat higher than the typical value for the outlying sheath observed by Rodriguez (1979), but the wave powers are actually within a factor of two when one takes into account the slope of the spectrum and the fact that the sheath measurements of Rodriguez (1979) do not extend to as low a frequency as the measurements of Gurnett *et al.* (1979) at the magnetopause. This seems to verify the observations of some observers that the waves at the magnetopause are typically much stronger than those in the magnetosphere, but are often scarcely distinguishable from the outlying magnetosheath.

Gurnett *et al.* (1979) reported perpendicular polarization of the wave electric field at the magnetopause, at least for the few examples for which a polarization measurement was possible. From combining their measurements of δB and δE over the 10 Hz–1 kHz range, they suggested that the electromagnetic component must be the whistler mode,

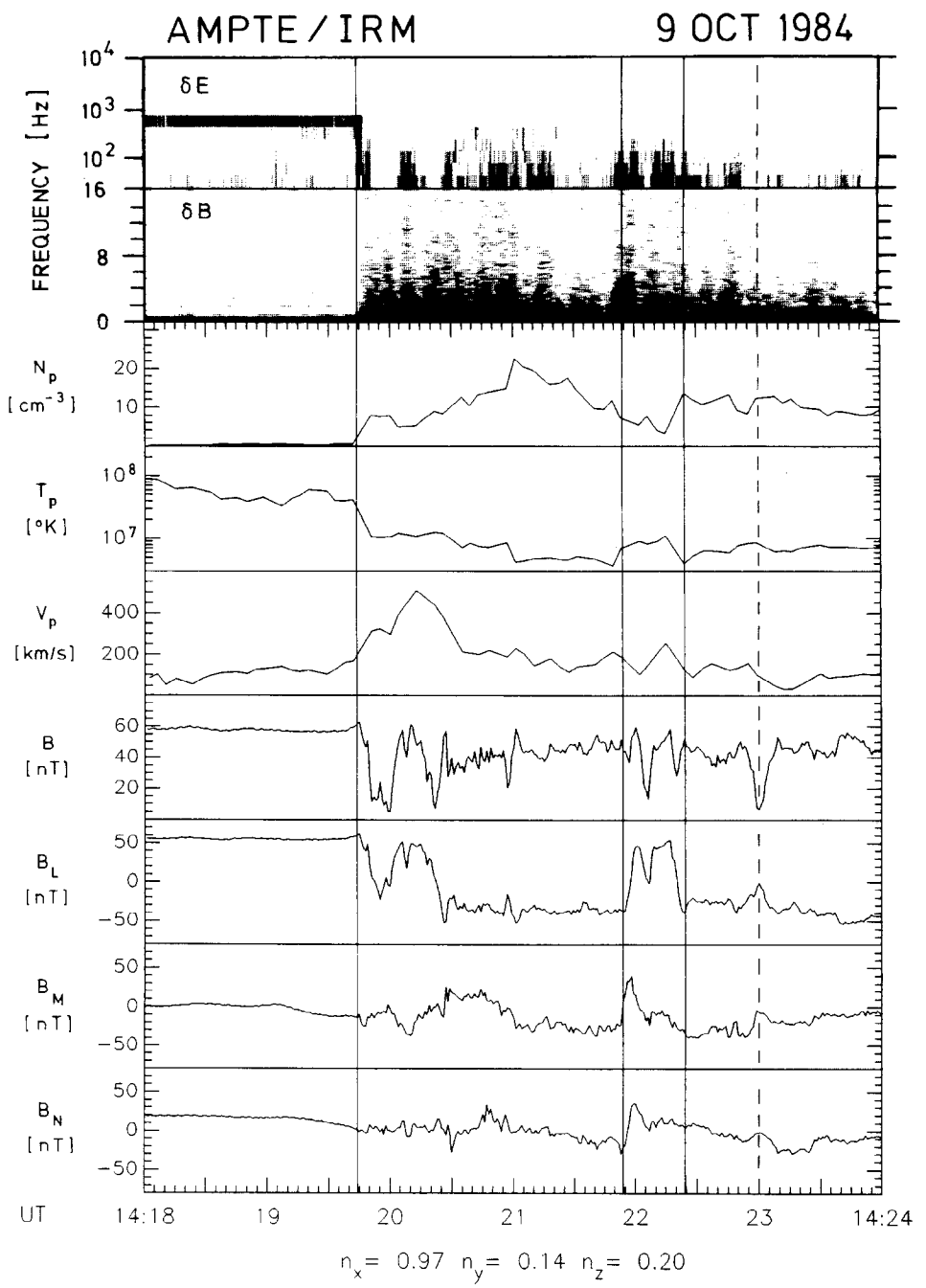

Fig. 1. AMPTE/IRM wave, particle and field data from three magnetopause crossings on October 9, 1984: (a) electric field fluctuations from 30 Hz to 10 kHz; (b) magnetic field fluctuations (0–16 Hz); (c) ion density; (d) ion temperature; (e–h) magnetic field magnitude and LMN components. The transformation to LMN coordinates is that used in Paschmann *et al.* (1986), and the *N*-direction is given in GSE coordinates at the bottom of the figure. Vertical lines indicate the positions of the three magnetopauses. A dashed vertical line indicates the location of a magnetic 'hole'.

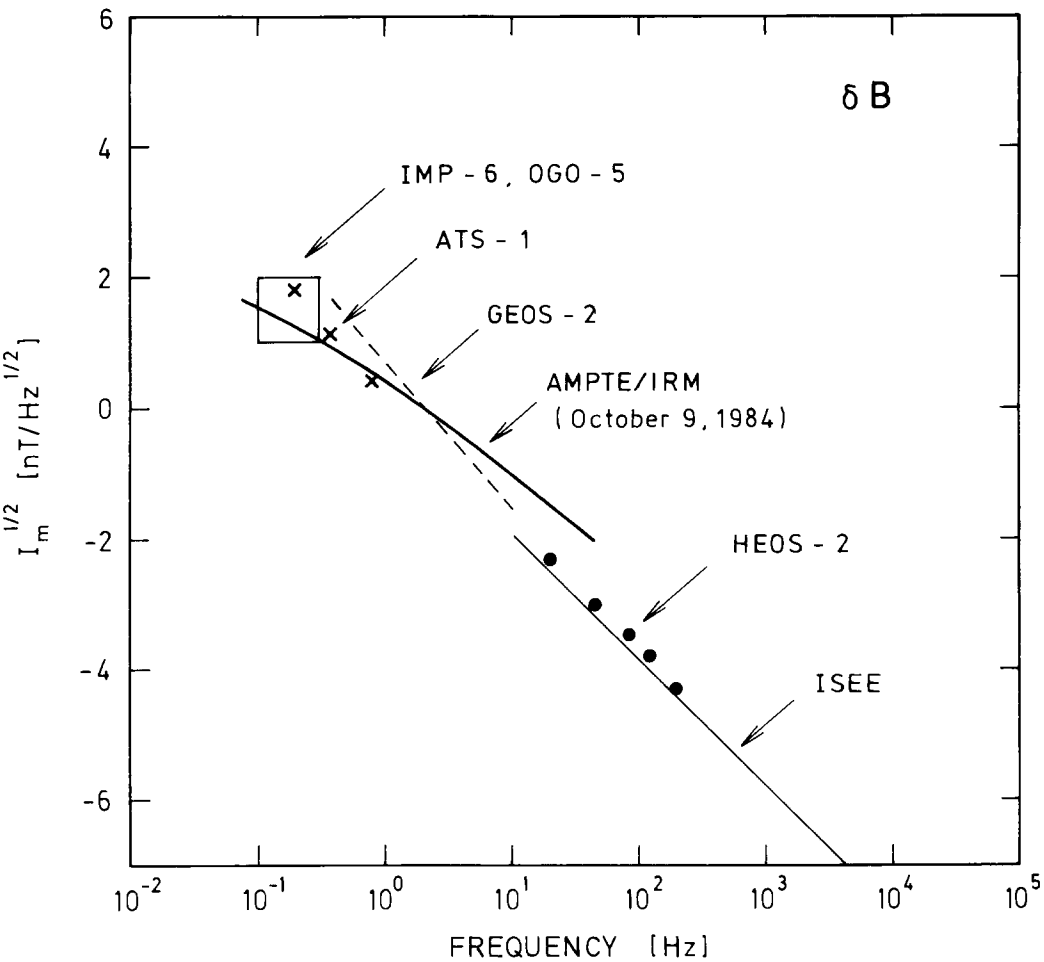

Fig. 2. The spectrum of magnetic fluctuations observed at the magnetopause from various different satellites (for references, see text).

but that a consideration of the whistler index of refraction implies a significant electrostatic component. Tsurutani *et al.* (1981) studied many more ISEE magnetopause crossings and found that the typical spectrum may be defined by $I_e \equiv \delta E^2/\varepsilon_0 = (3 \times 10^{-5}) f^{-2.8}\,\mathrm{V^2\,Hz^{-1}}$ for the frequency range 10 Hz–100 kHz. As with the magnetic field, the spectrum varies by up to an order of magnitude from case to case. Anderson *et al.* (1982) studied the morphology of the waves in detail from the ISEE crossings. They noted again little qualitative difference in the waves between the magnetopause, boundary layer, and FTE's. They observe spike-like waves at the magnetopause as well as in the boundary layer, FTE's, and outlying sheath, which resemble those reported by Rodriguez (1979).

The IRM data generally confirm the results of ISEE for the frequency range

30 Hz–100 kHz. Figure 3 shows the electric field spectrum measured by the IRM wave experiment on October 9, 1984, 14:20 UT, the first magnetopause crossing of Figure 1. Indicated is the spectrum exactly at the magnetopause current sheet as well as the average spectrum over a 30 s interval including the magnetopause. (The latter is somewhat lower in this example.) Also shown is the average electric field spectrum measured with the ISEE wave instrument (Tsurutani *et al.*, 1981). The IRM measures somewhat higher power, though Tsurutani *et al.* (1981) note that the variation from case to case is rather large, as is also clear from their Figure 3, so that the IRM example certainly falls within the range of ISEE observations.

In the October 9 case, the integrated amplitude of the electric field is about 10 mV m^{-1}. Following LaBelle *et al.* (1987), we can estimate the anomalous diffusion

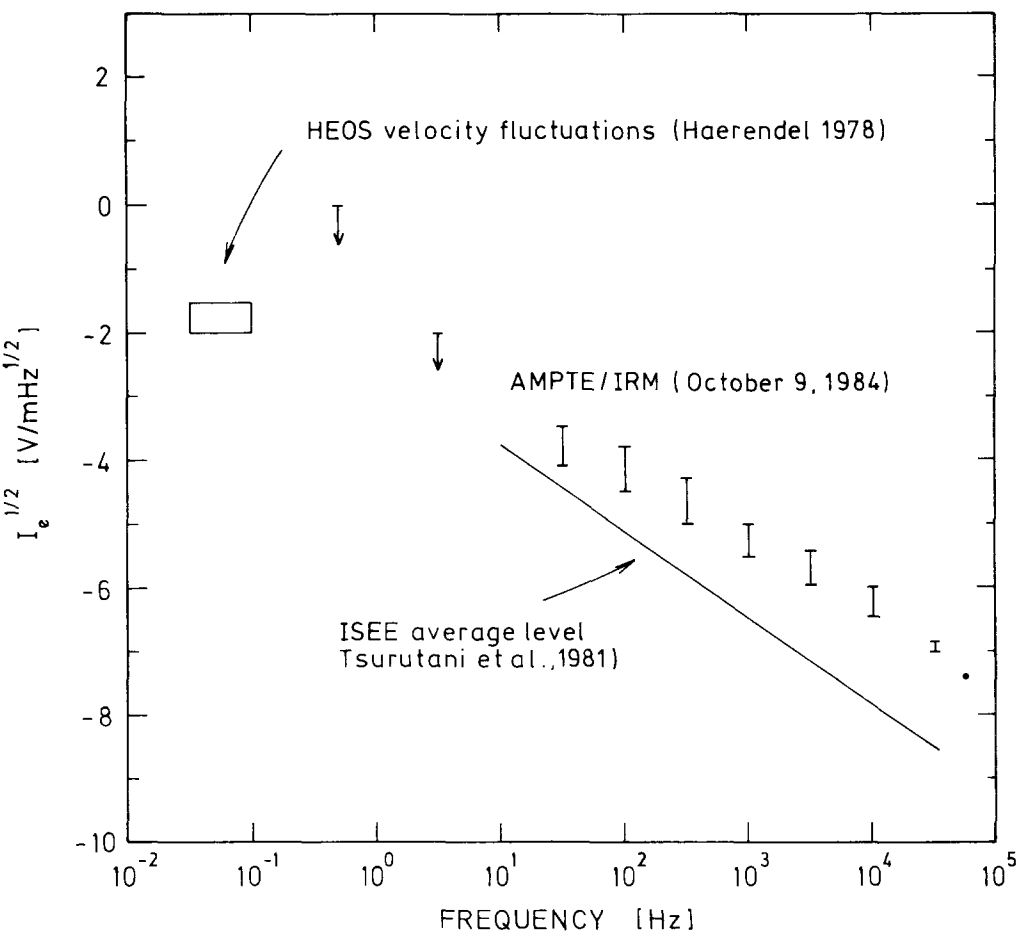

Fig. 3. The spectrum of electric fluctuations observed at the magnetopause from ISEE and from AMPTE/IRM. The IRM data comes from a single day; the maximum value at the magnetopause is shown, along with the spectrum averaged over the magnetopause region. The IRM data from below 30 Hz are only upper limits on the wave amplitude. Also shown is the typical value of electric field fluctuations below 0.1 Hz corresponding to the velocity fluctuations reported from the HEOS satellite (Haerendel, 1978).

associated with these waves assuming they are lower hybrid waves (Galeev, 1984); LaBelle *et al.* (1987) assume $10\ \text{mV m}^{-1}$ and find that D is approximately $2 \times 10^5\ \text{m}^2\ \text{s}^{-1}$. This implies diffusion times the order of 10^4 s if the diffusion region is 100 km thick. Thus, waves orders of magnitude stronger must characterize the magnetopause diffusion region if the anomalous collision rate associated with microturbulence is to provide the diffusion; we take up this problem in more detail below (Section 4.2).

At lower frequencies, the quasi-*dc* electric field fluctuations are considerably more difficult to measure than the magnetic field fluctuations in the same frequency range, because the double-probe experiments suffer from large errors in the *dc* field determination which are generally compounded by the low densities typical of the outer magnetosphere. In addition, the spin frequency of most satellites lies in the range 0–10 Hz and causes interference which can be difficult to remove. However, from the response of the IRM double-probe experiment during a large number of magnetopause crossings, we have computed upper limits to the wave field for the frequency ranges 0–1 and 1–4 Hz. These are indicated by downward arrows in Figure 3; they imply that the spectrum could continue to extend to lower frequencies with the same slope as determined by Tsurutani *et al.* (1981) but probably does not steepen significantly at low frequencies. From this, we can calculate an upper limit of approximately $40\ \text{mV m}^{-1}$ for the amplitude of the electric field integrated over 0.1 Hz–100 kHz.

Extending the spectrum of Tsurutani *et al.* (1981) to 0.1 Hz, we obtain an amplitude of about $5\ \text{mV m}^{-1}$ for the fluctuations at that frequency (assuming $\delta f/f \approx 1$); for a magnetic field of 100 nT (typical of the magnetopause), this implies fluctuations in drift velocity of $50\ \text{km s}^{-1}$ – not unreasonable for detection by drift detectors. Interestingly, Haerendel (1978) reviews HEOS measurements from the cusp-magnetosheath interface which show a layer of turbulent drifts with amplitudes up to $100\ \text{km s}^{-1}$. This represents a scale in between the large-scale Kelvin–Helmholtz-driven fluctuations and the microscopic structures we review here. The range of the HEOS intermediate-scale velocity measurements (converted to electric field using a reasonable magnetic field value) are shown in Figure 3 and clearly fall along the extension of the Tsurutani *et al.* (1981) spectra.

Haerendel (1978) interprets these fluctuations as turbulent eddies that develop along the magnetopause analogous to eddies in a fluid flowing past a boundary (Figure 4 from Haerendel (1978)). Possibly such a process injects energy at medium scales (≈ 0.1 Hz), which then cascades nonlinearly to shorter scales, leading to the observed electrostatic spectrum at frequencies a few Hz to kHz. Gurnett *et al.* (1979) noted that the featureless spectrum of δE would be expected from a cascade process. The electrostatic fluctuation spectrum observed in the satellite frame follows approximately an $I_e \sim f^{-8/3}$ power law; this corresponds to a two-dimensional k-spectrum of $k^{-11/3}$ if one assumes that spatial irregularities convect past the spacecraft (as discussed in LaBelle and Kelley, 1986). This is significantly steeper than the canonical slope of $-\frac{5}{3}$ for the energy cascade in the inertial subrange for hydromagnetic turbulence (Kolmogoroff, 1941; Kraichnan, 1967). Kraichnan (1982) arrives at a weak correction to this by applying renormalization theory. However, the spectrum which has been observed at the magnetopause

(Figures 2–3) probably corresponds to wavelengths shorter than the wavelength of energy input and, therefore, the appropriate process may be a forward cascade rather than an inverse cascade (if it is appropriate to speak of an inertial cascade at all, since there may be substantial energy input at intermediate and short scales as well). The slope may be steeper in the inertial range associated with a forward cascade; in experiments and simulations a large range of spectral indices have been reported (e.g., Kelley and Kintner, 1976; Fyfe and Montgomery, 1979; Hossain *et al.*, 1983). The observed spectrum does not fit the expected properties of a drift-wave cascade (Hasegawa and Mima, 1977, 1978).

In this model, a large or medium scale process could be ultimately the source for the electroscatic part of the spectrum observed at the magnetopause. The other portion of the spectrum, which consists of electromagnetic whistler mode waves, may arise from microscopic processes such as lower hybrid drift instability or ion cyclotron instability as suggested by previous research, with the source frequencies washed out by Doppler shifting as suggested by Gurnett *et al.* (1979). Alternatively, the whistler portion could be also generated through the cascade via coupling to the whistler mode when the cascade process reaches appropriate wavelengths. In this latter picture, virtually all of the turbulent layer at the magnetopause is generated by a cascade from the large scales. Most likely, however, a mixture of processes occurs.

3. Surveys of Plasma Waves at the Magnetopause

Tsurutani *et al.* (1981) performed a survey of 150 magnetopause crossings recognized from the ISEE plasma and magnetic field data. Although they did not show the results explicitly, they found no correlation between wave intensity and the change in magnetic field magnitude or direction across the magnetopause. Their survey included presumably the range of waves which they reported from ISEE: magnetic fluctuations from 10 Hz to 1 kHz, and electric fluctuations from 10 Hz to 100 kHz. Since the first years of ISEE, Perraut *et al.* (1979) and others have pointed out that most of the wave energy in the magnetopause spectrum is at lower frequencies (0–10 Hz). As a result, we have performed a smaller survey of IRM plasma wave observations in order to confirm the results of Tsurutani *et al.* (1981), to extend them to the lower-frequency waves, and to look for correlations with other magnetopause parameters.

Table I summarizes the data from 54 IRM magnetopause crossings taken from 32 different IRM orbits during Fall, 1984; 29 of these crossings correspond to large magnetic shear ($\geq 90°$), and many of these are magnetopause crossings previously identified by Paschmann *et al.* (1986). Low magnetic shear cases have to be detected using primarily the IRM temperature and density measurements and are naturally more difficult to recognize. Three magnetopause parameters have been recorded for each case: the magnetic shear, the change in magnetic field across the boundary, and the upstream plasma beta. (This last has been shown by Paschmann *et al.* (1986) to be related to reconnection.) If a distinct peak in the wave intensity is observed at the current layer, this intensity is recorded; otherwise, the wave intensities represent estimates of

the average intensity over a 30 s interval including the current layer. Three wave parameters are included: 0–1 Hz magnetic fluctuations, 1–4 Hz magnetic fluctuations, and 30–100 Hz electric field fluctuations. This last wave parameter falls within the frequency range sampled by Tsurutani *et al.* (1981). Blank entries in Table I indicate orbits for which particular wave parameters are not available.

In agreement with Tsurutani *et al.* (1981), we obtain no correlation between the wave parameters and magnetopause characteristics for the Fall 1984 IRM observations. For example, Figure 4 presents scatter plots of the δB (1–4 Hz) intensity plotted against magnetic shear angle, β_{upstream}, and ΔB. Furthermore, we find no correlation between magnetopause parameters and the slope of the δB-spectrum, as estimated from the difference between the 0–1 Hz and the 1–4 Hz wave intensities.

As noted above, even the maximum observed wave power does not correspond to the anomalous resistivity required for reconnection. Combined with the negative results of these surveys, this has three possible consequences for reconnection at the dayside magnetopause. First, perhaps the 'diffusion region' associated with reconnection is not characterized by any special wave characteristics, as if, for example, a large amount of microscopic wave-induced anomalous diffusion is not required for the reconnection. (We investigate this possibility in Section 4.3 below.) Second, perhaps the 'diffusion region' is exceedingly thin – less than a kilometer – such that satellite wave instruments with 1-s resolution see no trace of it. And third, it could be that the 'diffusion region' is thick enough to observe, but is limited enough in its other two dimensions so that the probability of encountering it within 40–150 magnetopause crossings is low.

Since theories of reconnection indicate a diffusion region with thickness the order of the ion inertial length or greater (≥ 100 km for the dayside magnetopause), we consider the second possibility to be unlikely. If we assume the third possibility, the negative survey results can enable us to put an upper limit on the size of the diffusion region. Since Paschmann *et al.* (1986) observe the flow signatures of reconnection on roughly 50% of the high-shear magnetopause crossings, we may assume that the x-line and its associated diffusion region extends in local time across most of the dayside magnetopause. (The x-line is either always present under high-shear conditions but extends over roughly half the local times, or it occurs half the time under high-shear conditions but occurs over all local times, or somewhere in between.) Hence, the negative survey results have important implications for the other dimension – the latitudinal extent of the diffusion region.

One could adopt a crude upper limit by assuming that the diffusion region lies with equal probability anywhere within 30° latitude of the subsolar point, and extends over half the dayside magnetopause. In this case, the probability of encountering the diffusion region on a given magnetopause crossing under high-shear conditions is given by $P = (\frac{1}{2})(\lambda_{\text{diff}}/60°)$, where λ_{diff} is the latitudinal width of the diffusion region. The probability of an encounter after N magnetopause crossings can then be roughly estimated as NP, provided that this product remains significantly less than unity. By setting the probability after N crossings to 50% to account for the fact that the diffusion region is not observed, we effectively obtain λ_{diff} and, hence, the upper limit on the size of the

TABLE I

IRM magnetopause crossings – Fall 1984

Date	Time	*R–E*	Lat.	LT	Beta	*B*	Angle	E1	B1	B2	B3
30 Aug., 1984	10:04	9.8	2.0	12.3	1.1	25	130	0.5			
30 Aug., 1984	10:05	9.8	2.0	12.3	1.1	25	130	1.0			
1 Sep., 1984	06:23	10.0	2.8	12.2	0.2	100	120	0.7	12.0	3.00	40.0
2 Sep., 1984	15:52	11.4	−19.0	15.1	0.5	0	30	1.5	0.5	0.50	15.0
4 Sep., 1984	15:05	7.6	−25.8	15.8	0.4	20	90	7.0	8.0	8.00	200.0
8 Sep., 1984	14:45	9.1	7.2	11.7	0.2	0	65	1.5	2.0	0.3	8.0
10 Sep., 1984	12:36	11.1	5.0	11.9	5.2	40	90	0.4	1.0	0.3	5.0
12 Sep., 1984	08:27	10.6	6.4	11.8	0.7	25	75	1.0	0.5	1.0	8.0
12 Sep., 1984	08:30	10.6	6.4	11.8	0.7	15	75	5.0	0.2	0.5	10.0
12 Sep., 1984	08:49	11.0	5.6	11.8	0.7	50	90	1.0	0.5	0.6	4.0
12 Sep., 1984	08:50	11.0	5.6	11.8	0.7	50	90	1.0	0.5	1.0	30.0
14 Sep., 1984	04:42	10.6	6.6	11.6	2.8	40	90	1.3	0.8	0.6	25.0
14 Sep., 1984	04:46	10.6	6.6	11.6	2.8	40	90	3.0	2.0	8.0	50.0
17 Sep., 1984	10:48	10.5	−22.0	14.2	0.4	5	30	0.5	0.2	0.3	2.0
17 Sep., 1984	10:57	10.3	−22.0	14.2	0.4	5	30	0.6	2.0	0.25	3.0
17 Sep., 1984	10:59	10.3	−22.0	14.2	0.2	0	30	0.9	1.2	0.15	2.0
19 Sep., 1984	16:10	8.8	11.4	11.6	0.8	35	45	1.3	1.0	1.00	50.0
21 Sep., 1984	13:01	9.5	12.5	11.1	1.5	35	90	1.0	1.0	2.00	100.0
23 Sep., 1984	00:24	9.5	−10.0	14.4	3.6	35	150	0.4		0.40	100.0
23 Sep., 1984	00:25	9.5	−10.0	14.4	3.6	35	30	0.4		1.00	50.0
23 Sep., 1984	00:27	9.5	−10.0	14.4	3.6	45	30	1.0		4.00	100.0
23 Sep., 1984	07:54	7.5	17.3	10.6	0.4	30	30	3.0	5.0	6.00	200.0
25 Sep., 1984	05:48	9.9	12.0	10.9	2.5	30	130	0.8	4.0	1.00	40.0
25 Sep., 1984	05:50	9.9	12.0	10.9	2.5	25	150	0.8	4.0	1.00	40.0
28 Sep., 1984	12:33	10.5	−16.4	13.6	4.4	50	105	1.5	4.0	1.00	20.0
6 Oct., 1984	06:17	8.2	19.0	9.9	0.4	5	30	4.0	0.8	0.60	20.0
6 Oct., 1984	06:20	8.2	19.0	9.9	0.4	10	30	1.5	0.2	0.40	2.0
8 Oct., 1984	05:31	10.8	13.5	10.2	5.4	45	180	2.0	3.0	1.00	30.0
9 Oct., 1984	14:07	10.1	−10.5	13.1	5.0	40	10	1.5	2.0	1.00	30.0
9 Oct., 1984	14:20	10.1	−10.5	13.1	1.3	45	30	2.0	6.0	1.50	50.0
11 Oct., 1984	11:36	9.0	−13.0	13.1	2.2	40	180	3.0			
11 Oct., 1984	11:38	9.0	−13.0	13.1	2.2	40	90	0.7	20.0	1.00	70.0
19 Oct., 1984	04:59	9.3	18.4	9.3	3.1	40	180	5.0	8.0	3.00	100.0
19 Oct., 1984	04:59	9.3	18.4	9.3	3.1	40	180	6.0	5.0	0.60	60.0
22 Oct., 1984	12:18	10.2	− 5.4	12.3	4.1	55	180	0.8		0.80	20.0
22 Oct., 1984	12:21	10.2	− 5.4	12.3	4.1	55	180	0.4		0.60	30.0
24 Oct., 1984	09:31	9.0	− 6.8	12.4	1.4	60	130	0.8	4.0	5.00	70.0
28 Oct., 1984	12:09	11.4	22.9	9.2	1.4	10	30	0.7	1.2	1.00	15.0
30 Oct., 1984	08:23	11.4	23.4	9.0	2.0	20	60	0.8	2.0	0.50	40.0
1 Nov., 1984	03:22	9.9	14.4	8.4	1.2	10	90	2.0	7.0	2.00	80.0
12 Nov., 1984	04:54	9.7	17.1	7.7	2.3	25	180	3.0	1.0	0.90	30.0
12 Nov., 1984	04:56	9.8	17.1	7.7	2.3	15	150	2.0	1.0	0.40	4.0
12 Nov., 1984	06:39	11.8	20.5	8.1	4.0	30	180	2.0	5.0	0.90	50.0
12 Nov., 1984	06:41	11.8	20.5	8.1	4.0	20	180	1.5		2.00	100.0
23 Nov., 1984	07:52	11.3	21.3	7.3	2.1	10	150	2.5	2.0	2.00	70.0
23 Nov., 1984	08:55	12.4	22.2	7.4	2.0	25	30	0.6	1.0	2.00	40.0
28 Nov., 1984	09:11	10.0	6.7	10.3	14.3	45	130	0.9	2.0		
30 Nov., 1984	07:39	7.8	3.2	10.5	0.5	0	30	5.0	2.0	0.30	10.0
9 Dec., 1984	10:38	11.0	7.9	9.4	1.5	15	0	0.6	0.7	0.80	15.0
9 Dec., 1984	10:39	11.0	7.9	9.4	1.5	15	0	1.0	0.9	0.50	15.0
22 Dec., 1984	09:13	10.0	5.1	8.7	5.4	50	0	2.0	6.0	10.00	10.0
22 Dec., 1984	09:27	9.8	5.1	8.7	5.8	45	30	1.0	2.0	8.00	20.0
27 Dec., 1984	21:56	10.1	−16.0	8.4	0.4	10	15	0.4	1.0	0.10	2.0
27 Dec., 1984	22:04	10.1	−16.0	8.4	0.8	15	0	1.2	2.0	3.00	200.0

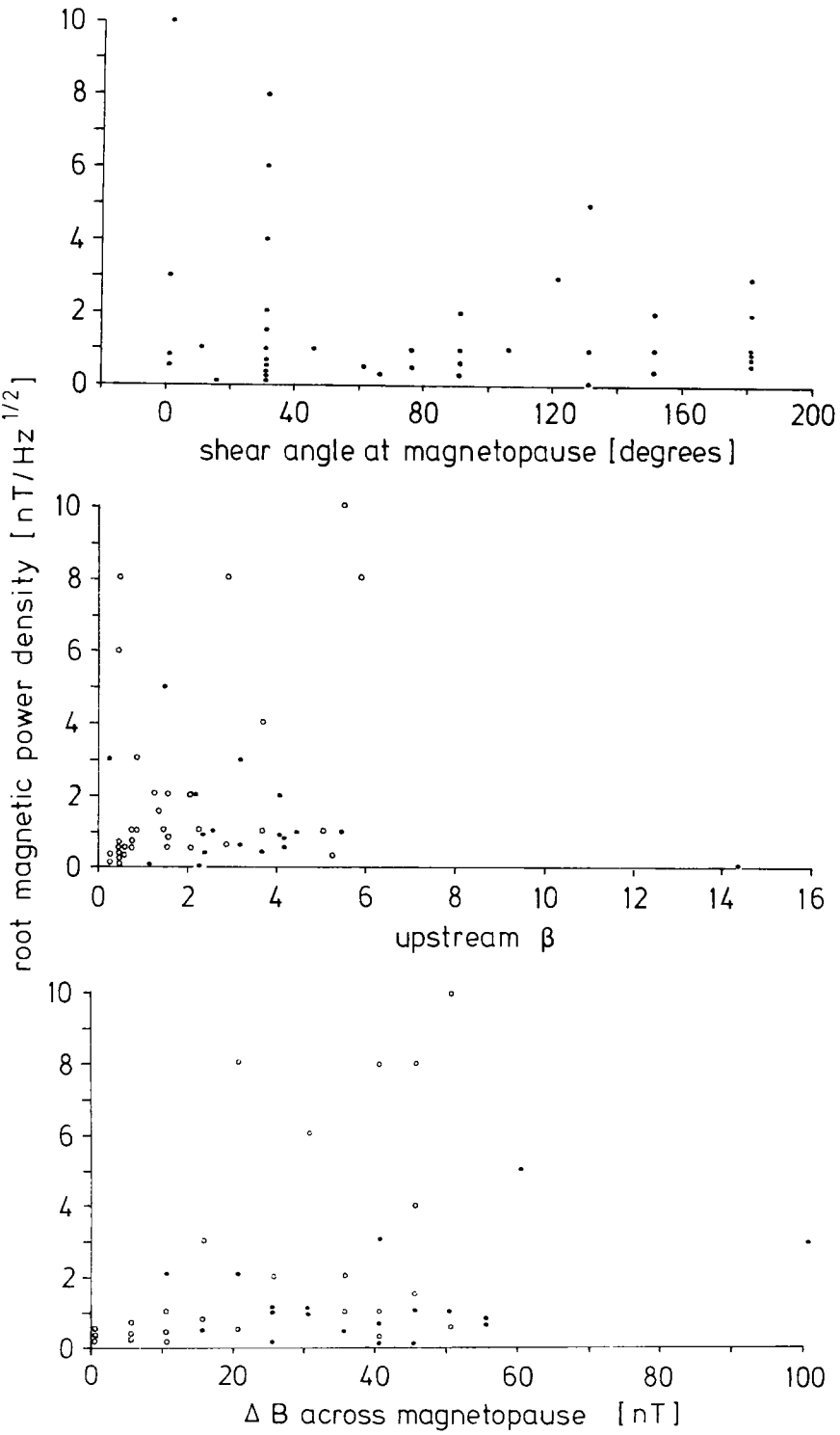
root magnetic power density [nT/Hz^1/2]
shear angle at magnetopause [degrees]
upstream β
Δ B across magnetopause [nT]

diffusion region, as a function of N. If we restrict ourselves to 'independent' magnetopause crossings (i.e., those from different orbits) with shear angle greater than 120°, then from Table I we find $N = 13$. This implies an upper limit of $\lambda_{\text{diff}} \leq 4.6°$, corresponding to approximately 5000 km. Tsurutani *et al.* (1981) do not report what fraction of their 150 dayside magnetopause crossings occur during large-shear conditions, but assuming that independent measurements under high-shear conditions occur in the same proportion as in the IRM data, we may increase N to 52, implying an upper limit for the diffusion region size of 1300 km.

To test this crude model, we adopt for the IRM data a more realistic model in which the probability is high near the subsolar point but decreases at local times away from noon. Specifically, we adopt the probability function:

$$P(LT) = \frac{1}{2} \frac{\lambda_{\text{diff}}}{\lambda_{LT}} , \tag{1}$$

where

$$\lambda_{LT} = \frac{360°}{24} (LT - 12) + 20° . \tag{2}$$

The factor $\frac{1}{2}$ comes from the fact that the x-line only covers half of local times in general, as discussed above. The first term in λ_{LT} assumes that the x-line has roughly equal probability of being oriented at any angle from 0–45 deg with respect to the ecliptic, and 20 deg is added (somewhat arbitrarily) to account for the fact that the probability is somewhat distributed even at noon. We note that the IRM high-shear magnetopause cases all fall within 10° of a cone of 45° centered on noon (Figure 1 of Paschmann *et al.*, 1986), so that this model should be applicable. Taking only the high-shear cases from Table I, we require that the probability of encountering the diffusion region be small,

$$P_{\text{total}} \approx \sum_{N} P(LT) \leq 0.5 , \tag{3}$$

where N is the number of cases. Taking the 13 high-shear examples of Table I, we obtain an upper limit of 3300 km, smaller than the 5000 km we obtained with the cruder method above. We conclude that the crude method provides if anything an overestimate of the diffusion region dimension, which must be limited to 3300 km in breadth if just the IRM survey data are used, and limited to the order of 1000 km when the ISEE survey of Tsurutani *et al.* (1981) is taken into account. Thus, it is not entirely surprising that satellite borne wave instruments have failed to see the strong wave turbulence which might characterize the diffusion region, and further comprehensive surveys of the wave

Fig. 4. The amplitude of magnetic fluctuations in the frequency range 1–4 Hz as a function of shear angle at the magnetopause, upstream plasma β, and ΔB across the magnetopause, compiled from 54 IRM magnetopause crossings. No correlation is observed between the wave parameters and the other magnetopause parameters.

data may enable us to put an even stronger limit on the dimensions of the diffusion region, if it indeed is characterized by distinct wave properties.

4. Theoretical Advances in Magnetopause Physics

4.1. Kelvin–Helmholtz instability

It is generally expected that plasma wave observations at the magnetopause answer the question of how the boundary layer can be formed by viscous or resistive interaction. Viscous interaction has been proposed originally by Axford and Hines (1961) to be responsible for the inertal magnetospheric convection. Any purely viscous process does, however, not lead to mass loading of the boundary layer from the magnetosheath. It merely leads to momentum coupling between the magnetosheath plasma and a plasma component already present in the boundary layer of the magnetosphere. Since the boundary layer seems to consist of magnetosheath plasma which has penetrated the magnetopause, the viscous coupling may be secondary in importance to the momentum transfer which occurs along with the mass loading of the boundary layer via particle diffusion, direct injection during reconnection, or some other process.

Recently, one model for such a momentum/mass coupling has been explored by Miura (1982, 1987) and Wu (1986), who perform numerical simulations of the magneto-hydrodynamic Kelvin–Helmholtz instability. This instability has been shown to create long wavelength plasma vortices at the magnetospheric boundary containing locally steep pressure and density gradients, thin current layers and magnetic vortices. The magnetic stresses in these vortices lead to a high anomalous viscosity which is shown by Miura (1987) to fully account for the magnetopause viscosity required to drive magnetospheric convection. (Mozer (1984) observes viscous effects at the duskside magnetopause and estimates that the actual viscosity is far too low to produce the typical magnetospheric convection – a result dependent on the specific conditions of his observation, for which the Kelvin–Helmholtz instability is stable (Miura, 1987).)

Figure 5 shows an example of a simulation of the Kelvin–Helmholtz instability at the magnetopause (Miura, 1987). The geometry of the model is shown in the upper left-hand corner; the model allows for shear in both the flow velocity and the magnetic field and also allows for inclined field inside and outside of the magnetosphere. The results shown correspond to the saturation of the instability at time $t = 120a/v_0$, where $2a$ is the shear length, and V_0 is the flow velocity in the sheath, which in this simulation corresponds to an Alfvénic Mach number of $M_A = V_0/v_A = 5$. A large eddy occurs at the magneto-sphere, deforming its shape locally and generating steep pressure gradients (lower left-hand corner); locally strong flows and current layers are also generated.

Though the Kelvin–Helmholtz instability contributes only to viscosity, it may also produce the medium scale eddies noted by Haerendel (1978), which in turn may serve (through a nonlinear cascade process) as the source of the wave energy at smaller scales. The observed low-frequency spectrum does not contradict this interpretation. (See discussion of Section 2.2). Such a cascading means that the Kelvin–Helmholtz vortices

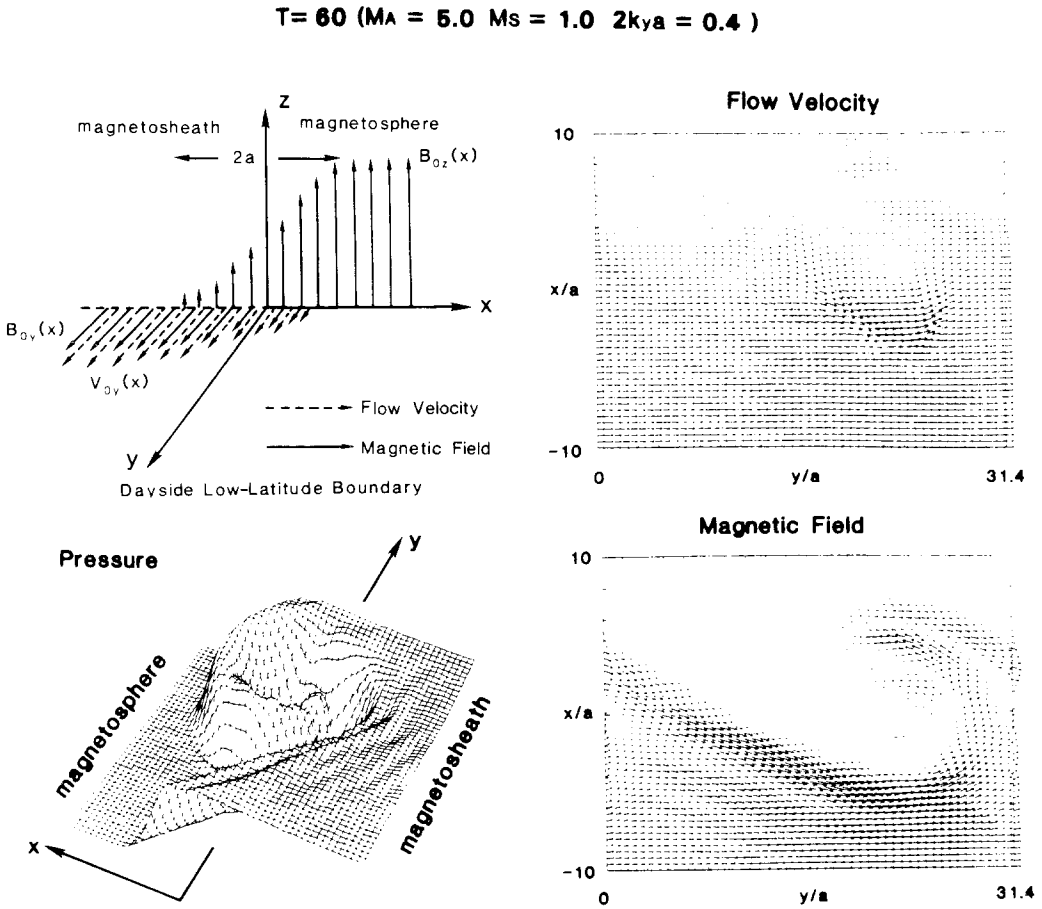

Fig. 5. Numerical simulation results of the Kelvin–Helmholtz instability at the magnetopause (Miura, 1987). The geometry is shown in the upper left corner. Flow velocity as well as magnetic field are allowed to have a shear. (The shear length is $2a$.) A pseudo-three-dimensional view of the pressure profile at saturation is shown (*bottom left*). The magnetosphere is to the left in this figure. The evolution of a large eddy and steep pressure gradients is obvious. Two-dimensional vector diagrams of the velocity and magnetic fields at saturation are given (*right-hand panels*). Strong current sheets as well as vortices evolve in the course of the instability.

decay to small scales possibly thereby driving other higher frequency wave modes. The full spectrum may then produce magnetic field migration (Section 4.3 below) or anomalous plasma diffusion (Section 4.2 below), either of which could load the boundary layer.

It is well known that the Kelvin–Helmholtz mode at the magnetopause should couple directly to Alfvén waves (Ohsawa *et al.*, 1976) which travel along the magnetic field lines down to the ionosphere. These waves may provide part of the low-frequency spectrum, but since little is known about the coupling efficiency for real conditions, it is impossible to estimate the contribution of these waves to the spectrum. Secondary effects of Alfvén

waves include current instabilities inside the magnetosphere which could dissipate part of the energy of the Kelvin–Helmholtz mode (e.g., Lysak and Hudson, 1987). However, since the fastest growing mode has a growth time considerably shorter than the Alfvénic travel time, the reaction of the reflection region or the ionosphere can probably be neglected.

Of greater importance is the evolution of the steep gradient regions in the Kelvin–Helmholtz vortices. Where these gradients become too strong, or where the currents become locally too strong, microinstabilities such as the modified two-stream instability or the lower hybrid drift instability can be excited. Anomalous resistivity then arises locally and gives rise to plasma diffusion or, in cases where the magnetic field is locally antiparallel, may even trigger the tearing mode instability and cause reconnection. These regions would be localized in space and could form the starting points for FTE's. If these regions are confined to well under 1000 km, they are rarely detected by satellites (see Section 3). In the next section we review the anomalous diffusion process which might occur in such localized regions.

4.2. Anomalous diffusion

Reconnection requires the presence of some nonlinear diffusion process to work in the diffusion region. Here we shall distinguish between two different kinds of reconnection. First, the process proposed by Dungey (1961) involves continuous reconnection at a neutral-point (x-point) on the dayside magnetopause. To provide diffusion of the magnetic field the resistivity has to be high near the x-point, within at least a small region where the diffusion takes place (diffusion region). Several papers discuss limitations on the linear size of the diffusion region (e.g., Vasyliunas, 1975; Haerendel, 1978, and references therein). Since the plasma in the magnetopause region is essentially collisionless, the diffusion must result from anomalous transport process associated with, for example, plasma waves. In this case, one should observe the highest plasma wave turbulence level at the diffusion region. Alternatively, the diffusion and, therefore, the x-point may be not steady-state but time-dependent. A second type is diffusive reconnection via the evolution of the collisionless tearing mode (Galeev *et al.*, 1986); this model is the subject of Section 4.3 below. Here we are concerned with the possible sources of anomalous collisions for the traditional picture of reconnection, be it 'steady-state' or 'patchy'.

For a magnetized plasma, the diffusion coefficient is given by (e.g., Ichimaru, 1973):

$$D_{\perp} = \rho_e^2 \nu_{an} \left(1 + \frac{T_i}{T_e}\right), \tag{4}$$

or, in the case that the plasma is non-magnetized, which may be applicable to the diffusion region since the field goes to zero at the x-point, the diffusion is given by

$$D_{\parallel} = \eta_{an}/\mu_0 = \left(\frac{c}{\omega_e}\right)^2 \nu_{an} . \tag{5}$$

In either case, ν_{an} represents the anomalous collision frequency due to the microscopic plasma turbulence, ρ_e is the electron gyro-radius, and η_{an} is the anomalous resistivity. In general, ν_{an} depends on wave power, but through a relation which is highly dependent on the dispersion relation for the particular waves which are excited (e.g., Galeev and Sagdeev, 1984). A simplified version of the general formula of the anomalous collision frequency is

$$\nu_{an} = \frac{\varepsilon_0 \delta E^2}{2 m_e n v_d} \left(\frac{\gamma_{\max}}{v_{\phi, \max}} \right). \tag{6}$$

We note that only current-driven waves result in anomalous resistivity, but there are still a host of possibilities. Some of these have been reviewed by Haerendel (1978) and Papadopoulos (1979). Here we review briefly three processes which have been proposed to generate the diffusion at the dayside magnetopause, and we present empirical calculations for upper limits on the diffusion coefficient from each.

Huba *et al.* (1977) were the first to suggest that lower hybrid waves may be important in reconnection; this wave mode appears especially promising since it involves high anomalous transport properties (Davidson and Krall, 1977; Davidson, 1978; Chen and Birdsall, 1983; Brackbill *et al.*, 1984). Lower hybrid waves can be excited either through the lower hybrid drift instability (LHDI) if only a density gradient is present (implying a diamagnetic current), or through the modified twostream instability (MTSI) if a current is also present. One problem is that they are damped by high beta (i.e., at the x-point itself!), but it has been suggested that they occur on the border of the diffusion region and nevertheless give rise to the required diffusion there. To estimate the anomalous collision frequency, we take the formula of Galeev (1982), simplified for the parameters of the magnetopause region (see LaBelle *et al.*, 1987):

$$\nu_{an} = \left(\frac{\pi}{8} \right)^{1/2} \left(\frac{m_i}{m_e} \right) \omega_{LH} \frac{\varepsilon_0 \delta E^2}{2 n T_i} . \tag{7}$$

Taking the observed wave power upper limit to be 10^{-3} V^2 m^{-2}, along with $B = 50$ nT, $n = 10$ cm^{-3}, $T_e = 25$ eV, and $T_i = 1$ keV implies $D = 1.3 \times 10^6$ m^2 s^{-1}. As discussed by LaBelle *et al.* (1987), for a diffusion region 100 km in extent this result implies a diffusion time of 7.6×10^3 s, somewhat too long to account for the reconnection rate at the dayside magnetopause. LaBelle *et al.* (1987) concluded that one possibility is that the diffusion region is not observed. This is obviously consistent with the survey results discussed in Section 3 above.

The highest diffusion coefficient is obtained assuming that the MTSI is responsible for the observed wave spectrum. This instability is a cousin of the LHDI but is driven by perpendicular current and has a slightly different dispersion relation (McBride *et al.*, 1972; Papadopoulos, 1979). The maximum growth rate is given by $\gamma_{\max} \approx \omega_{LH}/2$, the frequency by $\omega_{\max} \approx \sqrt{3}\, \omega_{LH}/2$, and the wavenumber by $k_{\max} \approx \sqrt{3}\, \omega_{LH}/v_d$. Inserting

these equations into (6), we obtain

$$\nu_{an} = \frac{\varepsilon_0 \delta E^2}{2 m_e n v_d^2} \omega_{LH} . \tag{8}$$

For the usual plasma and magnetic field parameters and upper limit for the wave power ($\delta E^2 \leq 10^{-3}\ \mathrm{V^2\,m^{-2}}$), this implies a maximum diffusion coefficient of $1.8 \times 10^7\ \mathrm{m^2\,s^{-1}}$, corresponding to a diffusion time of 560 s if the diffusion region is approximately 100 km thick.

Another possibility is to interpret the observed spectrum as electron-cyclotron drift waves. These have been proposed to account for the resistivity at the magnetopause (Lampe *et al.*, 1972; see review by Haerendel, 1978). The problem is that their theoretical saturation level is extremely low and leads to $D \approx 10^4\ \mathrm{m^2\,s^{-1}}$, too low to provide diffusion across a reasonably thick (order of ion inertial length) diffusion region. Here we shall make a quasi-empirical calculation assuming all of the observed wave power is in this mode, and arrive at an upper limit for D. We substitute the dispersion relation for the electron-cyclotron drift mode (Papadopoulos, 1979; Galeev and Sagdeev, 1984) into Equation (6), obtaining

$$\nu_{an} = \frac{\varepsilon_0 \delta E^2}{14 m_e n v_e^2} \omega_e \left(\frac{T_e}{T_i} \right) . \tag{9}$$

Taking again the wave power of $10^{-3}\ \mathrm{V^2\,m^{-2}}$, this implies a diffusion coefficient of $D \approx 3.2 \times 10^4\ \mathrm{m^2\,s^{-1}}$, or a diffusion time of 3.2×10^5 s (if again a diffusion region thickness of 100 km is assumed). This quasi-empirical diffusion coefficient is within a factor of three of the theoretical value and, hence, is too small by orders of magnitude.

A third possibility to provide the resistivity are current driven ion acoustic waves. Unfortunately, this mechanism requires $T_e \gg T_i$, which is not valid near the magnetopause, and therefore it has previously been ruled out (Coroniti and Eviatar, 1977). However, it is possible for the Buneman instability to act at the magnetopause. This instability cannot lead to enhanced collisions in a stationary state, as discussed, for example, by Haerendel (1978); however, it strongly heats electrons. Thus, we envision a two-step process in which the Buneman instability acts to heat the electrons to the point where the ion-acoustic instability can occur ($T_e \gg T_i$). To estimate the anomalous collision frequency due to the ion-acoustic waves, one can apply the Sagdeev formula (e.g., Galeev and Sagdeev, 1984):

$$\nu_{an} = \omega_e \frac{\varepsilon_0 \delta E^2}{2 n T_e} . \tag{10}$$

Taking the wave power as above ($10^{-3}\ \mathrm{V^2\,m^{-2}}$), with $T_e \geq T_i \approx 1$ keV, we obtain a diffusion coefficient of $D = 2.5 \times 10^6\ \mathrm{m^2\,s^{-1}}$, which is not much greater than that due to the other processes, yielding diffusion times the order of 4000 s.

To summarize the anomalous diffusion due to microturbulence, Figure 6 shows diffusion coefficients as a function of wave power, assuming four different wave modes

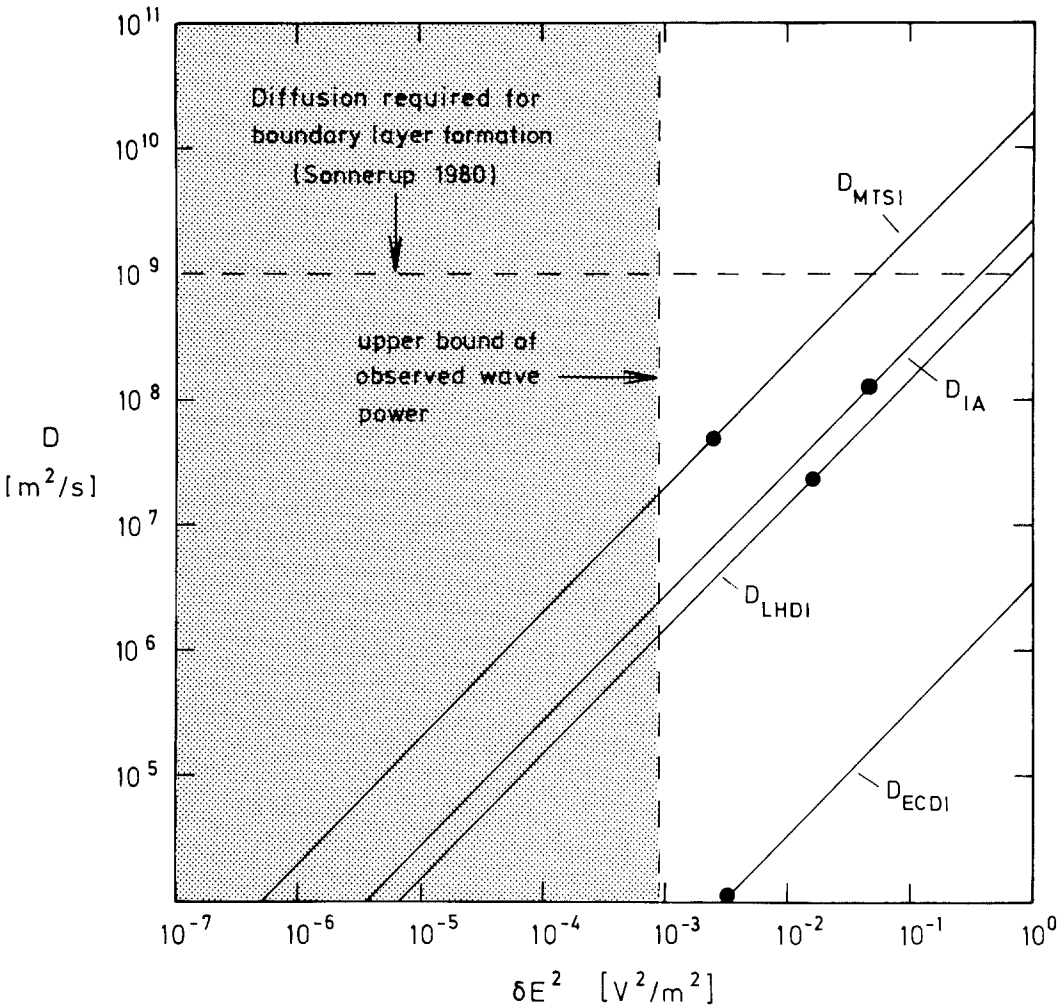

Fig. 6. The different microscopic diffusion coefficients (Table II) and their dependence on the total wave field power. The shaded region indicates the range of observed wave power. The dashed horizontal line at $D = 10^9\ m^2\ s^{-1}$ is the diffusion required for maintaining the boundary layer, according to the theory of Sonnerup (1980). Filled circles indicate the theoretical diffusion coefficients obtained from various nonlinear saturation models. These values are all larger than the quasi-empirical calculations based on observed wave powers, indicating that the theory tends to overestimate the wave level. All the diffusion coefficients, theoretical and quasi-empirical, fall well below the value $10^9\ m^2\ s^{-1}$.

(lower hybrid or MTSI, electron-cyclotron drift, and ion acoustic). The diffusion coefficients have been obtained from Equations (4) or (5), combined with the detailed dispersion characteristics of each mode; the equations are summarized in Table II. Since the diffusion coefficient is in all cases proportional to δE^2, the curves in Figure 6 are all straight lines. The range of the observed wave power is indicated by the shaded region and extends up to $\delta E^2 \approx 10^{-3}$, which corresponds to an upper limit of

Tab. 2: Anomalous Diffusion Coefficients

Mode	Diffusion Coefficient	References
IA	$D = (\frac{c}{\omega_e})^2 \omega_e \frac{\epsilon_0 \delta E^2}{2nT}$	
	$D^{th} = 10^{-2}(\frac{c}{\omega_e})^2 \omega_i (\frac{v_d}{c_s})(\frac{T_e}{T_i})$	Galeev & Sagdeev [1984]
LHDI	$D = (\frac{\pi}{8})^{\frac{1}{2}}(\frac{m_i}{m_e})(\frac{T_i}{T_e})\rho_e^2 \omega_{\mathrm{LH}} \frac{\epsilon_0 \delta E^2}{2nT_i}$	
	$D^{th} = 0.5\rho_e^2(\frac{m_i}{m_e})(\frac{v_d}{v_e})^2 \omega_{\mathrm{LH}}$	Huba & Papadopoulos [1978]
MTSI	$D = \rho_e^2 \omega_{\mathrm{LH}}(\frac{T_i}{T_e}) \frac{\epsilon_0 \delta E^2}{2nm_e v_d^2}$	
	$D^{th} = 0.1\rho_e^2(\frac{T_i}{T_e})\omega_{\mathrm{LH}}$	Papadopoulos [1979]
ECDI	$D = \frac{3}{7}\rho_e^2 \omega_e \frac{\epsilon_0 \delta E^2}{4nT_i}$	
	$D^{th} = 10^{-2}\rho_e^2 \Omega_e (\frac{v_d}{v_e})^3$	Haerendel [1978] Papadopoulos [1979]

30 mV m^{-1} for the total r.m.s. amplitude of the waves. The dashed horizontal line at $D = 10^9$ m^2 s^{-1} makes the value of D required on the average to maintain the boundary layer, according to the theory of Sonnerup (1980).

Table II furthermore provides purely theoretical estimates of the anomalous diffusion arising from the different wave modes, based on calculation of the wave saturation level.

These values are indicated in Figure 6 by filled circles. It is found that the theoretical values give wave powers consistently higher than the observed wave amplitudes but also fall short of the value required by Sonnerup's (1980) theory of the boundary layer. This indicates that the nonlinear theory either tends to overestimate the wave amplitude, or that the measurements so far are not sufficiently well-resolved in space or time to detect the waves of such high amplitudes.

Clearly, the observed waves give rise to diffusion coefficients no greater than 2×10^7, no matter which mechanism is envisioned. We conclude either: (1) The satellites have simply failed to observe the diffusion region, a reasonable possibility in light of Section 3; (2) there exists some not yet discovered microscopic process by which the observed spectrum can give higher diffusion; or (3) reconnection proceeds not according to the traditional model, in which the diffusion region is the order of an ion inertial length, but perhaps involves a much thinner diffusion region the order of an electron gyro-radius.

4.3. Magnetic field migration

The traditional model of a single x-point and associated diffusion region is not the only mechanism by which reconnection-driven momentum and mass transfer can occur across the magnetopause boundary. An alternative model, presented by Galeev *et al.* (1986), results from overlapping of a large number of tearing islands which evolve as a consequence of a kind of cascading process of the collisionless tearing mode at the magnetopause (Figure 7). Overlap of otherwise isolated small islands of width smaller than the width of the magnetopause current sheet may lead to a local breakthrough of the magnetic field from the magnetosphere into the magnetosheath and create channels for direct plasma inflow. (These might be FTE's.) Galeev *et al.* (1986) call this process 'percolation' of the magnetopause. Here we will refer to this process as 'magnetic field migration'.

Tearing mode instability is a very low-frequency process. The energy is injected at large scales and cascades to shorter scales; merging of magnetic 'islands' is an opposing process. There is the possibility that cascading and merging of islands lead to a stationary spectrum. Kleva (1982) estimated the thermal fluctuation level of the collisionless tearing mode. In a plasma of density n and magnetic shear length L_s the fluctuation amplitude is given by

$$\left(\frac{\delta B}{B}\right)^2 = \frac{\beta}{(4\pi)^2 n L_s}\left(\frac{\omega_e}{c}\right)^2. \tag{11}$$

At the magnetopause typically $L_s = 1000$ km, $B_0 = 100$ nT, $\beta = 1$, and $n = 1$–100 cm^{-3}, with the higher value of n belonging to the magnetosheath side of the boundary. The fluctuation level obtained is $(\delta B/B_0)^2 = 10^{-21}$–$10^{-24}$ and, hence, too small to be observed. The resulting diffusion leads to extremely long diffusion times. This result shows that the collisionless tearing mode in thermal equilibrium does not lead to noteworthy overlap of magnetic islands. For this to happen, a non-thermal spectrum of $\delta B/B$ is required.

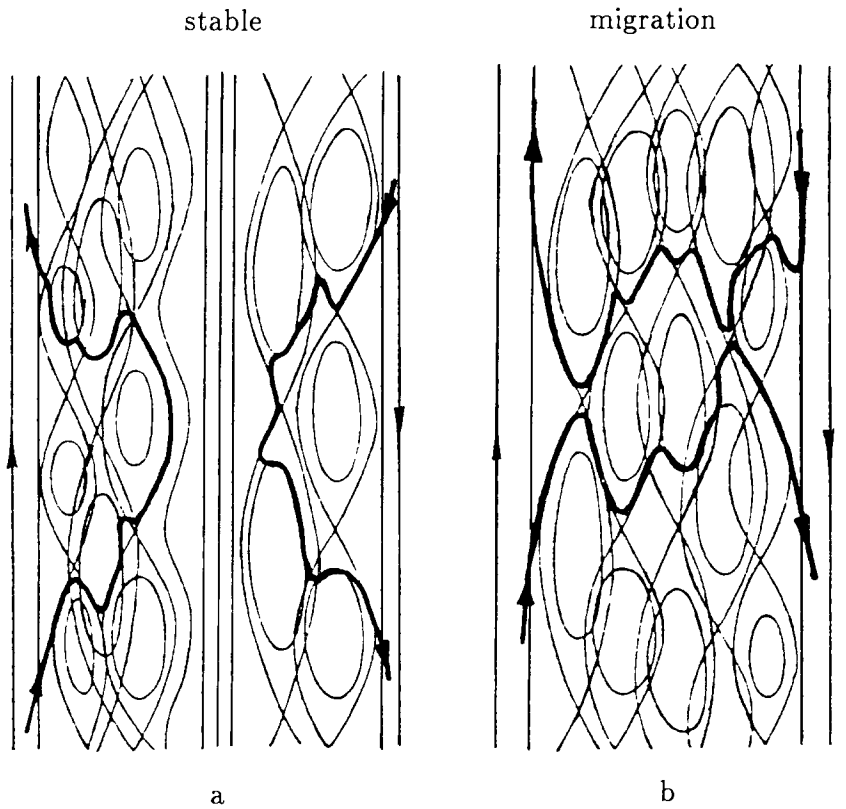

Fig. 7. Schematic of the magnetic field migration process at the magnetopause (after Galeev *et al.*, 1986): (a) the stable situation in which the tearing mode instability is weak, the islands do not overlap sufficiently to destroy the magnetic surfaces of the boundary, and the magnetic field lines cannot migrate across the magnetopause even for the case of anti-parallel magnetic fields; (b) the unstable case in which the tearing mode has destroyed the magnetic surfaces through overlapping of many small and large islands. Two magnetic field lines and their associated flux tubes have migrated across the magnetopause. Such a process may explain the formation of pairs of FTE's.

For a given measured spectrum $\delta B/B$, it is possible to determine an effective magnetic field migration diffusion coefficient (D_{MF}) (Rosenbluth *et al.*, 1966; Galeev *et al.*, 1986), as derived from an analogy to particle diffusion (Rechester and Rosenbluth, 1978; Galeev, 1984). This diffusion coefficient has a form similar to that of quasi-linear broadening (Dupree, 1967),

$$D_{MF} = \sum_{\mathbf{k}} \frac{|\delta B_{\mathbf{k}}^2|}{B^2} \int_0^\infty \mathrm{d}s \exp\left[- ik_{\|}(x)s - \frac{1}{3}\left(\frac{\mathrm{d}k_{\|}}{\mathrm{d}x}\right)^2 D_{MF} s^3 \right] \tag{12}$$

in which $k_{\|}(x(s)) = \mathbf{k} \cdot \mathbf{B}/B$ is the parallel wave number, s is the spatial coordinate along B, and where

$$\mathrm{d}x/\mathrm{d}s = (\delta B_{\mathbf{k}}/B) \cos(k_z z + k_y y) . \tag{13}$$

This diffusion coefficient has units of length. Following Galeev *et al.* (1986), we can roughly estimate its magnitude by neglecting the broadening term, which yields

$$D_{MF} = \pi \frac{\delta B^2}{B^2} \delta(k_\parallel(x)) \approx \frac{\delta B^2}{B^2 L_s} \left(\left| \frac{\mathrm{d}k_\parallel}{\mathrm{d}x} \right| \right)^{-1}, \tag{14}$$

where L_s is the shear length characteristic of the magnetopause boundary. The parallel wavenumber $k_\parallel$ is related to the length of the tearing mode islands, $k_\parallel = 2\pi/l$. We can estimate the derivative of $k_\parallel$ across the magnetopause as

$$\left| \frac{\mathrm{d}k_\parallel}{\mathrm{d}x} \right| \approx \frac{4\pi}{lL_s} . \tag{15}$$

The measured magnetic fluctuation spectrum (Section 2.1) suggests $(\delta B/B) \approx 0.1$–0.2; assuming $l = 1 - 2R_E$, we obtain $D_{MF} \approx 16$ km.

A particle diffusion coefficient can be determined from D_{MF} through the relation (Galeev *et al.*, 1986)

$$D_\perp = 0.75 v_e \left(\frac{m_e}{m_i} \right)^{1/2} \left(\frac{T_i}{T_e} \right) \left(\left| \frac{\mathrm{d} \ln k_\parallel}{\mathrm{d}x} \right| \rho_e \right)^{1/2} D_{MF} . \tag{16}$$

Substituting (14) and (15) into (16), we obtain

$$D_\perp = \frac{0.75}{4\pi} \left(\frac{m_e}{m_i} \right)^{1/2} \left(\frac{T_i}{T_e} \right) \left(\frac{\rho_e}{L_s} \right)^{1/2} l v_e \left(\frac{\delta B}{B} \right)^2 \tag{17}$$

in which we have assumed $T_i \gg T_e$. For $T_e \approx 25$ eV, $T_i \approx 1$ keV, and $L_s \approx 1000$ km, we obtain $D_{\perp e} \approx 2 \times 10^{10} (\delta B/B)^2$ m^2 s^{-1}. For the observed magnetic field fluctuation amplitude $(\delta B/B \approx 0.1$–$0.2)$, this implies $D_\perp \approx (2$–$4) \times 10^8$ m^2 s^{-1}. (The ambipolar diffusion coefficient would be about a factor of two lower.) This is somewhat below the particle diffusion of $\approx 10^9$ m^2 s^{-1} required to maintain the boundary layer according to the theory of Sonnerup (1980). For physical reasons, the diffusion must be below the absolute limit $v_e D_{MF} \approx 3 \times 10^{10}$ m^2 s^{-1}, as discussed by Galeev (1984). Note that this diffusion coefficient, related to the macroscopic process of magnetic field migration, is at least an order of magnitude greater than the anomalous diffusion associated with the same amplitude of lower hybrid waves or other microscopic processes (cf. Section 4.2).

We note the following properties of the above diffusion coefficient: (1) if the resonance broadening term is taken into account in a manner analogous to Dupree (1967), $D_\perp$ scales as $(\delta B/B)$ and is a factor 4–5 larger, which agrees better with the diffusion required by the theory of the boundary layer formation (Sonnerup, 1980); (2) the diffusion scales as $l/L_S^{1/2}$, implying a larger diffusion coefficient for large islands within a thin shear layer; and (3) the nearly continuous presence of the magnetic noise spectrum at the magnetopause, as reviewed in Sections 2 and 3 above, suggests that this kind of coupling continuously takes place at the magnetopause, leading to the occasional migration of field lines and building up the boundary layer. When the magnetic fields

on both sides of the boundary are not parallel, entire flux tubes may migrate, leading to FTE's. Actually, D_{MF} is proportional to $\tan\theta$, where θ is the half-angle between the magnetosheath magnetic field and that of the magnetosphere. Hence, the diffusion becomes vanishingly small for parallel fields.

The nonlinear tearing mode saturates when the average width of the islands is of the order of the ion gyroradius ρ_i (Galeev, 1984). The magnetic migration coefficient (14) then scales as:

$$D_{MF} \sim \rho_i^3 \left(L_s \left| \frac{\mathrm{d}k_\parallel}{\mathrm{d}x} \right| \right)^{-1} . \tag{18}$$

As a consequence, the perpendicular diffusion coefficient scales as $D_\perp \sim \rho_i^3 / L_s l$ (Galeev *et al.*, 1986), and since $\rho_i \sim v_i/B$, this diffusion coefficient scales with B as $D_\perp \sim 1/B^3$. This is precisely the scaling of the diffusion coefficient D_{TT} obtained by Tsurutani and Thorne (1982), which they assume to be proportional to the Bohm diffusion coefficient $(1/B)$ and to the wave power $(\delta B^2/B^2)$, and which consequently scales as $D_{TT} \sim B^{-3}$. Thus, it is not surprising that we obtain approximately the same diffusion coefficient as Gendrin (1983), who applies the diffusion coefficient of Tsurutani and Thorne (1982) to the low-frequency magnetic fluctuations at the magnetopause and obtains $D_\perp \approx 1000\ \mathrm{km^2\ s^{-1}}$, comparable to that required by Sonnerup's theory of the boundary layer (Sonnerup, 1980). However, Tsurutani and Thorne (1982) arrive at this result by applying the pitch angle scattering time (Kennel and Petschek, 1966) and assuming that this scattering time can be assumed as the anomalous collision time; this is actually an extreme upper bound on the efficiency of the particle diffusion. To our knowledge, no microscopic process has been proposed through which the observed wave spectrum can produce anomalous transport the order of $10^9\ \mathrm{m^2\ s^{-1}}$, as discussed above in Section 4.2. Rather, we conclude that magnetic field migration is a much more important diffusion process when the magnetic fields across the boundary are nonparallel, and the magnetic fluctuations which are important for this diffusion are the very lowest frequencies.

Even when the magnetic fields on either side of the magnetopause boundary are parallel, one can consider whether significant particle diffusion can arise from stochastic $\mathbf{E} \times \mathbf{B}$ scattering, if one assumes that the observed electrostatic spectrum is a turbulent cascade (i.e., consists of cells of convective motion rather than a coherent process such as wave steepening). Convective cells in two-dimensional plasma turbulence are known to give rise to strong cross-field diffusion (Vahala, 1973; Taylor and McNamara, 1971; Okuda, 1980). The diffusion coefficient can be calculated from the renormalized theory (Dupree, 1967) by assuming resonance broadening. The frequency spectrum measured by a spacecraft can be applied to determine this diffusion following LaBelle *et al.* (1968), assuming the usual conditions (time-stationary spatial irregularities convecting past the spacecraft, in which case the frequency in the spacecraft frame is proportional to the wavenumber). Assuming the convection velocity $v_{MS} \approx 100\ \mathrm{km\ s^{-1}}$, $B = 50\ \mathrm{nT}$, $\delta E^2 \sim k^{-2}$, and an outer scale of a few kilometers, we obtain $D \approx 10^9\ \mathrm{km^2\ s^{-1}}$. This is comparable to the result due to magnetic field migration. Since this mechanism applies

to parallel fields and therefore to closed magnetosphere conditions, it is possible that even under these conditions the electric field fluctuations are adequate to produce the diffusion required to maintain the boundary layer. This could explain the observed insensitivity of the boundary layer thickness to such parameters as the interplanetary magnetic field direction (Eastman and Hones, 1979). Again, the important waves are those with the largest scales (around 1 Hz in the above calculation). This mechanism requires that the observed electric field spectrum extends to the frequency range 0–10 Hz and actually represents a turbulent cascade, as would be the case, for example, if the source of the energy is a large scale process such as Kelvin–Helmholtz which then initiates a turbulent cascade to shorter scales. Of course, there could be input to the spectrum at shorter scales, or the spectrum may not extend to larger scales. (There is a crucial gap in the measurements in the range 0.1–10 Hz.) More experimental work is required to show whether convective transport is really an important process at the dayside magnetopause.

5. Summary

We commenced this paper by reviewing 20 years of wave measurements at the dayside magnetopause. The measurements point to a fairly consistent picture for the spectrum of fluctuations in both δB and δE. The δB spectrum takes the form $f^{-3.9}$ over the frequency range 10–1000 Hz and possibly flattens out to something like $f^{-2.5}$ at lower frequencies (1–10 Hz); the wave power is thus concentrated at low frequencies, and the integrated r.m.s. amplitude is about $\delta B \approx 10$ nT. The δE spectrum varies as approximately $f^{-2.7}$ in the range 10 Hz–100 kHz, but its dependence in the 0.1–10 Hz range is not known, although experiments do give upper limits which imply that the spectrum cannot be even steeper at these low frequencies. Drift velocity measurements show fluctuations below 0.1 Hz which may be continuous with the electric field spectrum at higher frequencies, but until better measurements are available, it is impossible to say for sure. The integrated r.m.s. amplitude in the measured spectrum above 10 Hz is about 3 mV m^{-1}. If the spectrum continues to lower frequencies with the same slope, the r.m.s. integrated amplitude may be an order of magnitude higher, however.

Theoretically, current-driven microinstabilities could be the source of the observed waves at the magnetopause current layer, and these could lead to anomalous diffusion. However, a quasi-empirical calculation based on the observed wave amplitudes shows that this anomalous diffusion due to various microscopic plasma waves is never high enough to explain either (1) the effective particle diffusion of 10^9 m^2 s^{-1} required to maintain the boundary layer according to the theory of Sonnerup (1980), or (2) reconnection-related diffusion occurring across a thickness the order of the ion inertial length or greater (≈ 100 km) within a time period of a few seconds as in the usual model. However, the number of cases which have until now been examined, although large, is not large enough to discount the possibility that during no observed case does a satellite actually penetrate the diffusion region – even assuming the diffusion region is as large as 1000 km in latitudinal extent.

However, it could be that the important diffusion processes at the dayside magnetopause are macroscopic, not microscopic. Such a process is the 'percolation of the magnetopause', or magnetic field migration, proposed by Galeev *et al.* (1986). For the observed r.m.s. amplitude of $\delta B/B \approx 0.1$–0.2, this mechanism provides 2–$4 \times 10^8\ \mathrm{m^2\ s^{-1}}$, quite a bit larger than any microscopic diffusion coefficient and within a factor of three of that needed to explain the boundary layer (Sonnerup, 1980). Convective transport (stochastic $\mathbf{E} \times \mathbf{B}$ diffusion) is another macroscopic diffusion process which could provide a diffusion coefficient as high as 10^9 (provided that the δE spectrum continues to lower frequencies than have been observed, and that this δE spectrum represents a turbulent cascade). If such a process is the dominant particle diffusion mechanism at the dayside magnetopause, this could explain the relative insensitivity of the boundary-layer thickness to the direction of the interplanetary field.

A great deal has been learned about the global characteristics of the boundary layer at the Earth's magnetopause and about the global consequences of reconnection at the dayside magnetopause; these have been the subjects of previous review papers (e.g., Willis, 1978; Cowley, 1982). Here we have dealt exclusively with waves at the magnetopause, which must play a major role in the detailed mechanisms of magnetopause physics. Much has been learned about the characteristics of the plasma waves at the magnetopause, but clearly much work remains to be done, both in the theoretical and in the experimental realm, before the processes of boundary layer formation or reconnection are understood in detail.

Acknowledgements

The authors would like to especially thank Hermann Lühr for preparing the IRM magnetic field data displayed in Figure 2. The AMPTE/IRM wave data was crucial to the preparation of this manuscript and owes its existence to the wave experiment team; R. R. Anderson, O. H. Bauer, D. A. Gurnett, G. Haerendel, B. Häusler, R. H. Holzworth, and H. Koons.

References

Anderson, K. A., Binsack, J. H., and Fairfield, D. H.: 1968, *J. Geophys. Res.* **73**, 2371.
Anderson, R. R., Harvey, C. C., Hoppe, M. M., Tsurutani, B. T., Eastman, T. E., and Etcheto, J.: 1982, *J. Geophys. Res.* **87**, 2087.
Aubry, M. P., Kivelson, M. G., and Russell, C. T.: 1971, *J. Geophys. Res.* **76**, 1673.
Axford, W. I. and Hines, C. O.: 1961, *Canadian J. Phys.* **39**, 1433.
Bahnsen, A.: 1978, *J. Atmospheric Terrest. Phys.* **40**, 235.
Brackbill, J. U., Forslund, D. W., Quest, K. B., and Winske, D.: 1984, *Phys. Fluids* **27**, 2682.
Chen, Y. J. and Birdsall, C. K.: 1983, *Phys. Fluids* **26**, 180.
Coroniti, F. V. and Eviatar, A.: 1977, *Astrophys. J. Suppl. Ser.* **33**, 189.
Cowley, S. W. H.: 1982, *Rev. Geophys. Space Phys.* **20**, 531.
Cummings, W. D. and Coleman, P. J., Jr.: 1968, *J. Geophys. Res.* **73**, 5699.
Davidson, R.: 1978, *Phys. Fluids* **21**, 1375.
Davidson, R. C. and Krall, N. C.: 1977, *Nucl. Fusion* **17**, 1313.
Dungey, J. W.: 1961, *Phys. Rev. Letters* **6**, 47.
Dupree, T. H.: 1967, *Phys. Fluids* **10**, 1049.

Eastman, T. E. and Hones, E. W., Jr.: 1979, *J. Geophys. Res.* **84**, 2019.
Eviatar, A. and Wolf, R. A.: 1968, *J. Geophys. Res.* **73**, 5561.
Fairfield, D. H.: 1971, *J. Geophys. Res.* **67**, 6700.
Fyfe, D. and Montgomery, D.: 1979, *Phys. Fluids* **22**, 246.
Galeev, A. A., Kuznetsova, M. M., and Zeleny, L. M.: 1986, *Space Sci. Rev.* **44**, 1.
Galeev, A. A.: 1982, 'Magnetospheric Tail Dynamics', in A. Nishida (ed.), *Magnetospheric Plasma Physics*, D. Reidel Publ. Comp., Dordrecht, Holland, p. 143.
Galeev, A. A.: 1984, 'Spontaneous Reconnection of Magnetic Field Lines in a Collisionless Plasma', in A. A. Galeev and R. N. Sudan (eds.), *Basic Plasma Physics*, Vol. 2, North-Holland, Amsterdam, p. 305.
Galeev, A. A. and Sagdeev, R. Z.: 1984, 'Current Instabilities and Anomalous Resistivity of Plasma', in A. A. Galeev and R. N. Sudan, *Handbook of Plasma Physics*, Vol. II, *Basic Plasma Physics*, North Holland, Amsterdam, p. 271.
Gendrin, R.: 1983, *Geophys. Res. Letters* **10**, 769.
Gurnett, D. A., Anderson, R. R., Tsurutani, B. T., Smith, E. J., Paschmann, G., Haerendel, G., Bame, S. J., and Russell, C. T.: 1979, *J. Geophys. Res.* **84**, 7043.
Haerendel, G.: 1978, *J. Atmospheric Terrest. Phys.* **40**, 343.
Haerendel, G., Paschmann, G., Sckopke, N., Rosenbauer, H., and Hedgecock, P. G.: 1978, *J. Geophys. Res.* **83**, 3195.
Hansen, A. M., Bahnsen, A., and D'Angelo, N.: 1976, *J. Geophys. Res.* **81**, 556.
Hasegawa, A. and Mima, K.: 1977, *Phys. Rev. Letters* **39**, 205.
Hasegawa, A. and Mima, K.: *Phys. Fluids* **21**, 87.
Holzer, R. E., McLeod, M. G., and Smith, E. J.: 1966, *J. Geophys. Res.* **71**, 1481.
Hossain, M., Mattheus, W. H., and Montgomery, D.: 1983, *J. Plasma Phys.* **30**, 479.
Huba, J. D., Gladd, N. T., and Papadopoulos, K.: 1977, *Geophys. Res. Letters* **4**, 125.
Hyde, R. S.: 1967, *Explorer 12 Magnetometer Observations of the Magnetosphere Boundary Region*, Publ. UNH 67–6 Department of Physics, University of New Hampshire, Durham.
Ichimaru, S.: 1973, *Basic Principles of Plasma Physics*, W. A. Benjamin, Inc., Reading, Mass.
Kelley, M. C. and Kintner, P. M.: 1976, *Astrophys. J.* **220**, 339.
Kennel, C. F. and Petschek, H. E.: 1966, *J. Geophys. Res.* **71**, 1.
Kleva, R. G.: 1982, *Phys. Fluids* **25**, 707.
Kolmogoroff, A. N.: 1941, *Compt. Rend. Acad. Sci. USSR* **30**, 301.
Kraichnan, R. H.: 1967. *Phys. Fluids* **10**, 1417.
Kraichnan, R. H.: 1982, *Phys. Rev.* **A25**, 3281.
LaBelle, J. and Kelley, M. C.: 1986, *J. Geophys. Res.* **91**, 7113.
LaBelle, J., Kelley, M. C., and Seyler, C. E.: 1986, *J. Geophys. Res.* **91**, 5513.
LaBelle, J., Treumann, R. A., Haerendel, G., Bauer, O. H., Paschmann, G., Baumjohann, W., Lühr, H., Anderson, R. R., Koons, H. C., and Holzworth, R. H.: 1987, *J. Geophys. Res.* **92**, 5827.
Lampe, M., Manheimer, W. M., McBride, J. B., Orens, J. H., Papadopoulos, K., Shanny, R., and Sudan, R. N.: 1972, *Phys. Fluids* **15**, 662.
Lühr, H. and Klöcker, N.: 1987, *Geophys. Res. Letters* **14**, 186.
Lysak, R. L. and Hudson, M. K.: 1987, *Laser and Particle Beams* **5**, 351.
McBride, J. B., Ott, E., Boris, J. P., and Orens, J. H.: 1972, *Phys. Fluids* **12**, 2367.
Miura, A.: 1982, *Phys. Rev. Letters* **49**, 779.
Miura, A.: 1987, *J. Geophys. Res.* **92**, 3195.
Mozer, F. S.: 1984, *Geophys. Res. Letters* **11**, 135.
Neugebauer, M., Russell, C. T., and Smith, E. J.: 1974, *J. Geophys. Res.* **79**, 499.
Ohsawa, Y., Nozaki, K., and Hasegawa, A.: 1976, *Phys. Fluids* **19**, 1139.
Okuda, H.: 1980, *Phys. Fluids* **23**, 498.
Papadopoulos, K.: 1979, 'The Role of Microturbulence on Collisionless Reconnection', in S. I. Akasofu (ed.), *Dynamics in the Magnetosphere*, D. Reidel Publ. Co., Dordrecht, Holland, 289.
Paschmann, G., Haerendel, G., Papamastorakis, I., Sckopke, N., Bame, S. J., Gosling, J. T., and Russell, C. T.: 1982, *J. Geophys. Res.* **87**, 2159.
Paschmann, G., Sckopke, N., Haerendel, G., Papamastorakis, I., Bame, S. J., Asbridge, J. R., Gosling, J. T., Hones, E. W., Jr., and Tech, E. R.: 1979, *Space Sci. Rev.* **22**,, 717.
Paschmann, G., Papamastorakis, I., Baumjohann, W., Sckopke, N., Carlson, C. W., Sonnerup, B. U. Ö, and Lühr, H.: 1986, *J. Geophys. Res.* **91**, 11099.

Perraut, S., Gendrin, R., Robert, P., and Roux, A.: 1979, *Magnetic Pulsations Observed Onboard Geos-2 in the ULF Range During Multiple Magnetopause Crossings*, ESA/SP-148, p. 113.
Rechester, A. B. and Rosenbluth, M. N.: 1978, *Phys. Rev. Letters* **40**, 38.
Rezeau, L., Perraut, S., and Roux, A.: 1986, *Geophys. Res. Letters* **13**, 1093.
Rodriguez, P.: 1979, *J. Geophys. Res.* **84**, 917.
Rosenbluth, M. N., Sagdeev, R. Z., Taylor, J. B., and Zaslavsky, G. M.: 1966, *Nucl. Fusion* **6**, 297.
Russell, C. T. and Elphic, R. C.: 1978, *Space Sci. Rev.* **22**, 681.
Scarf, F. L., Fredricks, R. W., Neugebauer, M., and Russell, C. T.: 1974, *J. Geophys. Res.* **79**, 511.
Sckopke, N., Paschmann, G., Haerendel, G., Sonnerup, B. U. Ö., Bame, S. J., Forbes, T. G., Hones, E. W., Jr., and Russell, C. T.: 1981, *J. Geophys. Res.* **86**, 2099.
Smith, E. J. and Davis, L.: 1970, *J. Geophys. Res.* **75**, 1233.
Sonnerup, B. U. Ö.: 1980, *J. Geophys. Res.* **85**, 2017.
Sonnerup, B. U. Ö., Paschmann, G., Papamastorakis, I., Sckopke, N., Haerendel, G., Bame, S. J., Asbridge, J. R., Gosling, J. T., and Russell, C. T.: 1981, *J. Geophys. Res.* **86**, 10049.
Taylor, J. B. and McNamara, B.: 1971, *Phys. Fluids* **14**, 1492.
Treumann, R. A., LaBelle, J., Bauer, O. H., Haerendel, G., Paschmann, G., Baumjohann, W., Lühr, H., Anderson, R. R., Gurnett, D. A., Koons, H. C., and Holzworth, R.: 1986, *Wave Observations in Association with Magnetic Holes in the Vicinity of the Magnetopause*, EOS Trans. AGU 67, p. 353.
Tsurutani, B. T., Smith, E. J., Thorne, R. M., Anderson, R. R., Gurnett, D. A., Parks, G. K., Lin, C. S., and Russell, C. T.: 1981, *Geophys. Res. Letters* **8**, 183.
Tsurutani, B. and Thorne, R. M.: 1982, *Geophys. Res. Letters* **9**, 1247.
Vahala, G.: 1973, *Phys. Fluids* **16**, 1876.
Vasyliunas, V. M.: 1975, *Rev. Geophys.* **13**, 303.
Willis, D. M.: 1978, *J. Atmospheric Terrest. Phys.* **40**, 301.
Wu, C. C.: 1986, *J. Geophys. Res.* **91**, 3042.